THE JOURNAL OF PHYSICAL CHEMISTRY B

Article

pubs.acs.org/JPCB

Dynamics of Dihydrogen Bonding in Aqueous Solutions of Sodium Borohydride

Chiara H. Giammanco, Patrick L. Kramer, and Michael D. Fayer*

Department of Chemistry, Stanford University, Stanford, California 94305, United States

Supporting Information

ABSTRACT: Dihydrogen bonding occurs between protonic and hydridic hydrogens which are bound to the corresponding electron withdrawing or donating groups. This type of interaction can lead to novel reactivity and dynamic behavior. This paper examines the dynamics experienced by both borohydride and its dihydrogen-bound water solvent using 2D-IR vibrational echo and IR pump−probe spectroscopies, as well as FT-IR linear absorption experiments. Experiments are conducted on the triply degenerate B−H stretching mode and the O−D stretch of dilute HOD in the water solvent. While the B−H stretch absorption is well separated from the broad absorption band of the OD of HOD in the bulk of the water solution, the absorption of the ODs hydrogen bonded to BHs overlaps substantially with the absorption of ODs in the bulk H_2O solution. A subtraction technique is used to separate out the anion-associated OD dynamics from that of the bulk solution. It is found that both the water and borohydride undergo similar spectral diffusion dynamics, and these are very similar to those of HOD in bulk water. Because the B−H stretch is triply degenerate, the IR pump−probe anisotropy decays very rapidly, but the decay is not caused by the physical reorientation of the BH_4^- anions. Spectral diffusion occurs on a time scale longer than the anisotropy decay, demonstrating that spectral diffusion is not yet complete even when the transition dipole has completely randomized. To prevent chemical decomposition of the BH_4^-, 1 M NaOH was added to stabilize the system. 2D-IR experiments on the OD stretch of HOD in the NaOH/water liquid (no borohydride) show that the NaOH has a negligible effect on the bulk water dynamics.

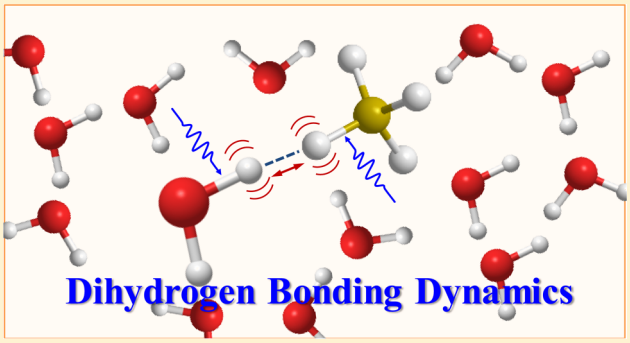

I. INTRODUCTION

In this paper, we examine the dynamics of borohydride (BH_4^-) in water from the perspectives of both the anion and the water using ultrafast two-dimensional infrared (2D-IR) spectroscopy and IR pump−probe experiments. The dynamics of water molecules interacting with (hydrogen bonded to) anions is a subject that has received a great deal of attention.[1−4] Borohydride provides the opportunity to examine the anion/water dynamics from the perspective of the anion by studying the B−H stretch using ultrafast IR experiments. It was also possible to look at the dynamics from the water perspective by making measurements on water hydroxyls that are hydrogen bonded to borohydride anions. In addition to the opportunity of measuring the dynamics of an anion hydrogen bonded to water from both sides of the hydrogen bond, the borohydride/water system is interesting because of the special nature of borohydride−water hydrogen bonds, that is, dihydrogen bonds.

Hydrogen bonding and hydrogen bond dynamics in liquids and other media have been under active investigation for decades because hydrogen bonds are involved in a vast number of phenomena and processes. Hydrogen bonds are intimately involved in proton transport in systems ranging from bulk water[5,6] to the nanoscopic channels of fuel cell membranes.[7,8] Hydrogen bonds are important in many biological systems. DNA strands are held together by hydrogen bonds;[9] enzymes have hydrogen bonds in their coordination sites;[10] sugars are coordinated by hydrogen bonds.[11] Hydrogen bonds in aqueous solutions govern many dynamical processes. The ability of water's hydrogen bonds to rapidly rearrange (∼2 ps time scale) is important in protein folding,[11,12] solvation of ions,[13−19] and many other processes.

Hydrogen bonds occur between a hydrogen bond donor, typically a hydrogen with a partial positive charge that is bonded to a more electronegative element such as oxygen, and a hydrogen bond acceptor which can be a lone pair of an electronegative element, the π electrons of an aromatic ring or multiple bond, or a transition metal center. A special case of hydrogen bonding has also been observed and has been the subject of recent study, the dihydrogen bond.

The dihydrogen bond was first postulated to explain vibrational spectra of amine−borane complexes in solution, which changed with concentration.[20,21] Earlier work[22,23] had observed vibrational spectral changes without recognizing that they were indicative of a special type of hydrogen bonding.

Received: December 13, 2014
Revised: January 28, 2015
Published: January 30, 2015

DOI: 10.1021/jp512426y
J. Phys. Chem. B 2015, 119, 3546−3559

Because of the relatively low electronegativity of boron, the borane hydrogens have partial negative charges. This partial negative charge allows the hydrogens to act as hydrogen bond acceptors, in contrast to the usual situation of, e.g., a hydroxyl, which acts as a hydrogen bond donor. The B−H in these amine−borane complexes interacts with the partial positively charged hydrogen covalently bound to the nitrogen. This interaction was confirmed via X-ray diffraction, which showed short B−H--HN contact. The association energy was measured to be 1.7−3.5 kcal/mol by variable temperature FT-IR.[24] Later work found that the bond lengths were in the range of 1.7−2.2 Å and occurred with B−H--(HN) angles of 95°−120°.[25,26] This places dihydrogen bonds on the same length and energy scale as conventional hydrogen bonds, but the geometries are more bent. When the borane was changed to the negatively charged borohydride, association energies increased to 2.3−6.5 kcal/mol.[27−29]

The phenomenon of dihydrogen bonding, however, is not unique to boron-containing species. Dihydrogen bonding often occurs with various transition metal hydrides. Those that have been studied extensively[25,30−33] include iridium, rhenium, and ruthenium, but dihydrogen bonding has also been seen with aluminum,[34] iron,[35] gallium, molybdenum, osmium, tungsten, and lithium metal centers.[36] These bonds are particularly bent, and the coordinating protonic hydrogen associates more with the σ-bond electrons rather than the hydridic hydrogen itself. Dihydrogen bonding with a transition metal hydride has been shown to contribute to their activity as catalysts. For example, dihydrogen bonding occurs in intermediates in the reactions of organoaluminum hydrides.[34] Dihydrogen bonding can also activate the reaction of H_2 leaving by leading to the formation of η^2-H_2.[30] In some complexes the presence of dihydrogen bonds may be responsible for stabilization against disproportionation.[37] Dihydrogen bonds control the reactivity and the selectivity of such reactions as hydrogen exchange, alcoholysis, and aminolysis, hydrogen evolution, and hydride reduction.[38] Dihydrogen bonding has also been proposed as a topochemical control while other reactions occur.[39,40] Thus, understanding the nature and the dynamics of dihydrogen bonds is important for a wide range of systems.

This paper focuses on the dynamics of borohydride dihydrogen bonds with water. Given the ubiquity of water as a solvent and the widespread use of borohydride as a reducing agent, the borohydride/water system is important in its own right, but it is also useful in understanding dihydrogen bond dynamics. It has been shown that reductions with borohydride can be controlled selectively and the rate can be tuned based on manipulating the dihydrogen interactions.[41,42] Basic aqueous solutions of borohydride have also been proposed as a hydrogen storage mechanism[43] and for use in fuel cells.[44] Thus, the water and borohydride system presents a fairly simple system to study hydrogen bonding, but it also has direct relevance to a variety of systems and processes. From neutron[36] and X-ray diffraction[45] experiments, the structure of water interacting with borohydride in the crystal $NaBH_4{\cdot}2H_2O$ is known. The hydrogen−hydrogen distances are 1.8−1.9 Å, which is much shorter than twice the van der Waals radius of a hydrogen atom (2.4 Å), a characteristic of dihydrogen bonding. The bonding angles are bent more than is observed in regular "linear" hydrogen bonding, and the hydroxyls point toward the middle of the B−H bond.[36] However, the hydroxyls are in fact bonding with the hydrogen itself and not the B−H σ-bond[45] as has been reported for some metal hydrides. These bent angles might lead to different dynamics in liquid water if they are maintained in the liquid phase. One MD simulation of the liquid water−borohydride system[46] has suggested that water does coordinate with a bent B−H−HO angle, although the simulation did not fully reproduce the experimental NEXAFS data. Higher level simulations could improve our understanding of this fascinating system and the nature of these dihydrogen bonds. Moreover, this paper provides measurements of dynamics that can be compared to the results of simulations providing a stringent test of the simulations. Previous work has looked extensively at the dynamics of water around various salts[1−4,13−19] and the hydrogen bonding in water itself.[47−55] Through comparisons to these systems, the dynamics of water associated with borohydride will report on the distinct nature of dihydrogen bonding.

2D-IR vibrational echo experiments were used to measure spectral diffusion of the B−H stretch of borohydride and the hydroxyl stretch of water. Spectral diffusion, which is the time dependent evolution of the frequency of the vibration under study, is caused by structural evolution of the system. For pure bulk water, 2D-IR experiments and simulations show that spectral diffusion is caused by very local hydrogen bond length fluctuation (∼0.4 fs time scale) and the total rearrangement of the hydrogen bond network (∼1.7 ps time scale).[47,56] Borohydride in water undergoes chemical decomposition by reducing water to produce H_2 gas. The H_2 gas bubbles in the samples interfere with the experiments. To essentially eliminate the decomposition on the time scale of the measurements, the experiments were conducted in aqueous solutions of 1 M NaOH (pH = 14). 2D-IR spectral diffusion measurements on the water hydroxyl stretch in the 1 M NaOH solution (no borohydride) are compared to experiments on pure water. It was found that the 1 M NaOH solution has the same spectral diffusion dynamics as pure bulk water within experimental error. Then 2D-IR experiments are performed on the B−H stretch at ∼2260 cm^{-1} and on the hydroxyl of water molecules hydrogen bonded to the borohydride. The OD stretch (∼2580 cm^{-1}) of dilute HOD in H_2O is investigated rather than H_2O to eliminate vibrational excitation transfer.[57−61] The results show that the dynamics of the B−H stretch and the stretch of OD hydrogen bonded to borohydride are almost the same and very close to those of bulk water.

II. EXPERIMENTAL PROCEDURES

Sodium borohydride and sodium hydroxide were purchased from Fisher Scientific and used without further purification. For the samples in which the water dynamics were monitored, the vibrational probe was the O−D stretch of 5% HOD in H_2O. The water was prepared by adding a small amount of D_2O to deionized ultra filtered water to produce a solution that was 5% HOD. This is a low enough concentration to avoid perturbing the H_2O solution dynamics and to avoid vibrational excitation transfer.[58−63] Salt solutions were prepared by weight. Sample cells were assembled by sandwiching the solution between two CaF_2 windows separated by a Teflon spacer. Infrared spectra were taken with a Thermo Scientific Nicolet 6700 FT-IR spectrometer. The spectrum of a sample without the vibrational probe was also taken, under identical conditions, and is used to subtract the background. When the B−H stretch was probed, the concentration of borohydride was kept below 1 M to ensure that vibrational excitation transfer between molecules was minimal.

DOI: 10.1021/jp512426y
J. Phys. Chem. B 2015, 119, 3546−3559

2D-IR spectra and IR pump−probe measurements were recorded using an experimental setup, for which the layout and procedures have been described in detail previously.[64] Briefly, a Ti:sapphire oscillator/regenerative amplifier system was run at a 1 kHz repetition rate and pumped an optical parametric amplifier (OPA). The signal and idler output of the OPA were difference-frequency mixed in a $AgGaS_2$ crystal to create ∼4 μm, ∼70 fs mid-IR pulses. The mid-IR beams propagated in an enclosure that was purged with air scrubbed of water and carbon dioxide to minimize absorption of the IR. Despite this, some carbon dioxide remained in the setup and so data around its absorption, ∼2350 cm^{-1}, were not included in the data analysis. The IR light was collimated and then split into two beams for the pump−probe experiments or four beams for the vibrational echo measurements. For the pump−probe experiments, the pump was rotated 45° relative to the probe and chopped. The two beams crossed in the sample, and the probe was resolved either parallel or perpendicular to the pump beam by a computer controlled polarizer. In the vibrational echo experiments, three IR pulses—the third of which is chopped—impinged on the sample in a box CARS geometry and stimulated the emission of the vibrational echo in the phase-matched direction. The echo was heterodyned with a fourth pulse. The signal (probe or echo) was dispersed by a monochromator employed as a spectrograph and detected on a 32 pixel, liquid nitrogen cooled, mercury−cadmium−telluride array.

Since borohydride in neutral water reacts quite rapidly, the solutions were adjusted to pH 14 using sodium hydroxide. The addition of NaOH significantly slows the reduction of water and subsequent liberation of hydrogen gas so that the concentrations in solution remain constant and no new species are produced over the course of the experiment.[65,66] However, the evolution of hydrogen gas still occurs and the formation of bubbles in the sample cells requires that they be remade every 1−2 days to prevent scattering of the laser beam from the bubbles. Each individual experiment was completed within this time scale.

III. RESULTS AND DISCUSSION

Linear and nonlinear time-resolved spectroscopies were used to interrogate the system of borohydride in water. Two different vibrational probes were employed: the asymmetric B−H stretch of the borohydride and the O−D stretch of HOD in H_2O with the ODs bound to the B−H's. The measurements permitted the observation of the dihydrogen bond dynamics from the perspectives of both partners.

A. Absorption Spectra. The O−D stretch of HOD is essentially a local mode. It gives rise to a broad FT-IR spectrum because of the large number of hydrogen bonding configurations present in water. Stronger hydrogen bonding with the HOD will result in absorption shifted to the red side of the band, and HODs with weak hydrogen bounds will absorb on the blue side of the band.

We want to determine the spectrum of the OD stretch for ODs that are hydrogen bonded to BHs. To do this, it is necessary to eliminate the other contributions to the spectrum, which are ODs bound to H_2O and the large tail of the B−H stretch spectrum of borohydride centered at 2262 cm^{-1} (see below). In Figure 1, the blue spectrum is for the OD stretch of HOD in 1 M NaOH solution. It was obtained by subtracting the spectrum of water/NaOH from the spectrum with 5% HOD. Unsubtracted FT-IR spectra can be found in the Supporting Information. Prior to subtraction, two spectra were normalized to the water combination band to eliminate path length differences. The resulting spectrum is centered at the same frequency, 2509 cm^{-1}, as the spectrum without NaOH, but it is slightly broader. The amplitude of the spectrum shown in the figure is from the fit discussed below.

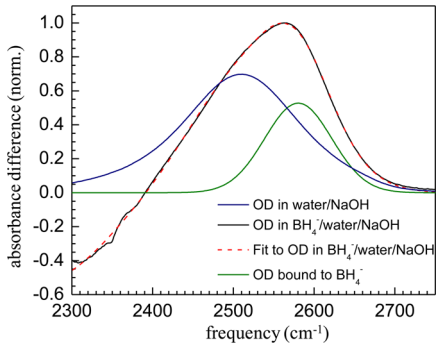

Figure 1. FT-IR spectrum of the OD stretch of HOD in 8:1 H_2O/$NaBH_4$ in pH 14 aqueous solution (black curve). The spectrum is fit to the sum of a scaled spectrum of the OD stretch in a solution without borohydride (blue curve), a Gaussian for the borohydride associated ODs (green curve), and a Gaussian for the residual portion of the B−H stretch (not shown, center frequency 2262 cm^{-1}). The dashed red curve is the fit.

The black spectrum shows the OD stretch region but this time with borohydride in the solution. It was obtained by subtracting the spectrum of the solution with borohydride without HOD from the spectrum with HOD. The sample without HOD had a slightly higher borohydride concentration, which after subtraction produced the negative-going region at frequencies lower than ∼2400 cm^{-1}. The small wiggle in the spectrum at ∼2350 cm^{-1} is residual CO_2 absorption. The peak of the total spectrum is shifted well to the blue compared to the spectrum of OD in water/NaOH (blue spectrum) that does not have borohydride in the solution.

To obtain the spectrum of the ODs bound to BHs, the following procedure was used. The black spectrum was fit by varying only the amplitude of the blue spectrum, adjusting the parameters of a Gaussian shifted well to red (with peak fixed at 2264 cm^{-1}) to account for the negative going portion of the black spectrum, and varying the parameters of a Gaussian on the blue side of the line, which is the desired spectrum of the ODs bound to BHs. The dashed red line is the resulting fit to the black spectrum. The fit reproduces the spectrum almost perfectly. The green curve is the desired spectrum of the OD stretch for ODs bound to BHs. It should be noted that this fit is not unique, and slight differences in the center frequency and width of the green curve can be obtained if other parameters are varied, but all the fits are very similar and show the same behavior. The principal use of the extracted green spectrum is to determine the region of the total spectrum that has a substantial contribution from ODs bound to borohydride. Therefore, the small differences that can occur in fitting the spectrum are not important.

The blue shift of the absorption spectrum of OD hydroxyls bound to anions has been reported and originates from hydroxyls that form weaker hydrogen bonds than they would have in pure bulk water.[1−4] The blue shift due to BH_4^- is larger than observed for ODs in sodium bromide solution.[67] The bromide anion is similar in size to borohydride, as it has a calculated radius for the isolated anion of ∼2.0 Å versus ∼1.9 Å

DOI: 10.1021/jp512426y
J. Phys. Chem. B 2015, 119, 3546−3559

for borohydride. The larger shift for ODs bound to BHs could be due to the different charge distributions of the two anions, but may also arise from the nature of the dihydrogen bond. Dihydrogen bonds in some cases have been found to be as much as 20% weaker than similar hydrogen bonds.[68] However, dihydrogen bonds can also become shorter when heavier isotopes of hydrogen are involved,[69−71] which may also affect the magnitude of the blue shift. Regardless of the mechanism, ODs bound to borohydride are shifted substantially blue from ODs bound to H_2O in bulk water. It should be noted that the green curve shown in Figure 1 was taken to be Gaussian in shape in the fit. With this assumption the resulting fit to the total spectrum is excellent (red dashed curve). However, the 2D-IR data discussed below show that there is a sizable Lorentzian component. The true line shape is a Voigt that is dominated by the Gaussian contribution.

Figure 2 presents the background-subtracted FT-IR spectrum of the B−H stretching region of 1 M sodium borohydride. To

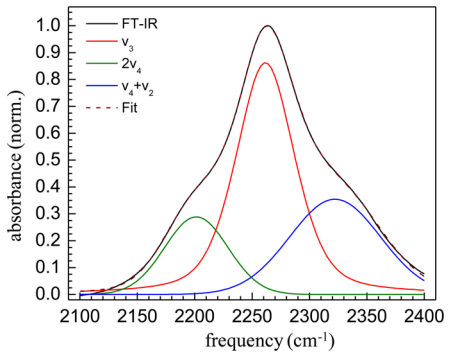

Figure 2. FT-IR spectrum of the B−H stretching region of borohydride (black curve) fit (red dashed curve) with three Gaussians (green, red, and blue solid curves). Borohydride has a triply degenerate vibration centered at 2262 cm^{-1}, with Fermi resonance enhanced shoulders from two quanta of the bend ($2\nu_4$) and a mixing of the bend with a Raman active mode ($\nu_4 + \nu_2$).

obtain the B−H spectrum, the spectrum of pH 14 water was subtracted from that of a pH 14 water solution with 1 M sodium borohydride. There are four B−H stretches. Because of the tetrahedral symmetry, three linear combinations of the stretches give rise to the triply degenerate asymmetric IR active modes (ν_3) and one to the Raman active mode (ν_1). There is a central peak in the spectrum shown in Figure 2 and two large shoulders. Only the central peak is of interest in this paper, as it corresponds to the triply degenerate asymmetric stretch of borohydride. The side peaks are most likely a 2-quanta overtone of the bend ($2\nu_4$) and a combination band of the bend and a Raman active mode ($\nu_4 + \nu_2$). This assignment is made in analogy with the assignment of the crystal spectrum[72,73] and borohydride in liquid ammonia.[74] The transitions that give rise to the shoulders would not have strong enough absorptions to be readily observed, but they have Fermi resonances with the very strong IR active asymmetric stretch, which gives them oscillator strength.[73]

Because every molecule in solution can contribute to the absorption spectrum, the effect of the hydroxide (which was added to stabilize the borohydride) was considered. Figure 3 shows the spectrum of the OD stretch of HOD in 1 M NaOH solution (red curve) and in pure bulk water (black curve). The spectra of the corresponding solutions but with no HOD were subtracted from the spectra with HOD. The shift in frequency

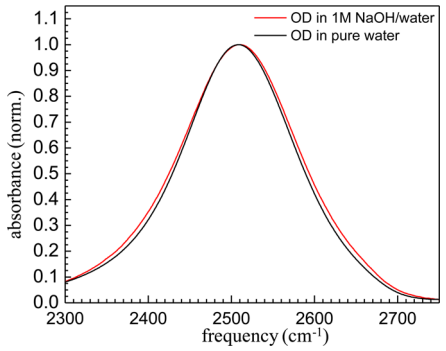

Figure 3. FT-IR spectrum of the OD stretch of HOD in 1 M NaOH (pH 14) in water (red curve) is slightly broader than that of the OD stretch in bulk water (black curve).

of the spectrum with NaOH is negligible, but the addition of hydroxide does cause a small broadening. No extra peaks or shoulders appear because the hydroxide is at a fairly low concentration. At higher concentrations the effect of the hydroxide on the spectrum as well as on the dynamics of the water molecules is significant.[75,76] It was also determined if the hydroxide affected the borohydride B−H spectrum. FT-IR spectra were taken at pH 13 (0.1 M NaOH) with and without sodium borohydride and subtracted as above. The spectrum at pH 13 is identical within error to the spectrum at pH 14 (data not shown). Therefore, the NaOH does not influence the borohydride spectrum.

B. Population Relaxation. The population relaxation (vibrational lifetime) data are extracted from the pump−probe signal by setting the polarization of the pump pulse at 45° relative to the horizontal probe and then resolving the polarization of the probe signal parallel $S_{\|}(t)$ and perpendicular $S_{\perp}(t)$ to the pump. These signals can be expressed in terms of population relaxation, $P(t)$, and the second Legendre polynomial orientational correlation function, $C_2(t)$.

$$S_{\|} = P(t)[1 + 0.8C_2(t)] \quad (1)$$

$$S_{\perp} = P(t)[1 - 0.4C_2(t)] \quad (2)$$

The normalized population relaxation is given by

$$P(t) = (S_{\|}(t) + 2S_{\perp}(t))/3 \quad (3)$$

The background sodium hydroxide produces a small signal, and this is subtracted from the data before the parallel and perpendicular signals are combined.[77,78] Because vibrational relaxation deposits a small amount of heat into the sample, there is a constant isotropic signal at a long time due to a temperature-dependent spectral shift. This heating term is removed to yield heating-free data.[54,79] At early times, the decay of the nonresonant signal interferes with the signal from the resonant vibrations. Thus, only the data after 200 fs is used.

Figure 4A shows the population decays for the OD stretch of HOD in three solutions: pure water, water with NaOH (1 M), and water with NaOH (1 M) and $NaBH_4$ (8 molecules of water per borohydride, ~7 M). In bulk water the lifetime of HOD is a single exponential decay with a time constant of 1.8 ps.[79−81] When the sodium hydroxide is added, the lifetime becomes biexponential with a fast time constant of 0.3 ± 0.1 ps and a long time constant of 2.1 ± 0.1 ps. When the borohydride is added the lifetime again fits to a biexponential with a long time constant of 2.1 ps, but the amplitude of the short time constant

DOI: 10.1021/jp512426y
J. Phys. Chem. B 2015, 119, 3546−3559

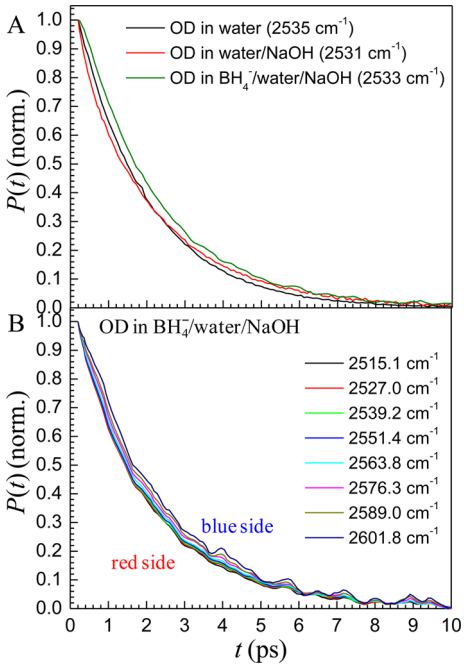

Figure 4. (A) Normalized $P(t)$ decays of the OD stretch of HOD in pure water (black curve), in 1 M NaOH solution (red curve), and in $NaBH_4$ (8 water molecules per $NaBH_4$) and 1 M NaOH solution (green curve). The decays are almost the same. (B) Normalized $P(t)$ decays of the OD stretch of HOD in 8:1 $H_2O/NaBH_4$ in pH 14 solution at various wavelengths across the absorption band. There is very little wavelength dependence of the vibrational lifetime. There is a very fast low amplitude component caused by spectral diffusion. See text.

(0.2 ± 0.1 ps) goes from positive to negative across the band. We attribute this short time constant to spectral diffusion appearing in the population decay. In the presence of unequal pumping the isotropic signal is no longer the pure population relaxation. The addition of both NaOH and $NaBH_4$ broadens the spectrum and means that the laser bandwidth will be less able to pump all wavelengths evenly, leading to underpumped wings. These wavelengths will become filled in as spectral diffusion occurs and so their "population" will appear to grow while the wavelengths at the center of the band will lose amplitude and appear to undergo a faster additional population decay process. Figure 4B shows the OD stretch population decays as a function of wavelength in the solution of water with NaOH and $NaBH_4$, which is the system used in the 2D-IR experiments. There is a very small wavelength dependence, due to the varying amplitude of the fast time component. However, the bulk of the $P(t)$ decay (population relaxation) is wavelength independent. Looking at the decomposed spectrum in Figure 1 (green curve and blue curve), the wavelengths in Figure 4B move from the red side where the population is dominated by ODs hydrogen bonded to water molecules through the region to the blue where the spectrum has a large contribution from ODs bound to BHs. The addition of sodium borohydride has little effect on the OD lifetime. Thus, the relaxation of the OD stretch of this concentrated sodium borohydride solution is unexpectedly similar to that of bulk water.

The vibrational population relaxation depends on the environment in which a molecule is located. The medium surrounding a molecule influences the coupling and the density of states of the modes that will take up the energy from the initially excited vibration.[82] In bulk water the OD stretch energy quickly dissipates into many combinations of lower frequency modes, including bending, torsion, and bath modes, which sum to the initial vibrational energy.[83] If there are two distinct environments for the molecules of interest in solution, these environments will give rise to different lifetimes unless, by coincidence, different environments produce the same lifetime. Generally, distinct environments will produce different absorption spectra. For systems that have broad absorption spectra, the spectral shifts can be too small to be resolved. However, the existence of different environments can be manifested in the wavelength dependence of the population relaxation. If there are two environments that give rise to two different lifetimes, the pump−probe decays will be biexponential and the amplitude of the two components will change with the detection wavelength across the vibrational line.

In Figure 4B there is at most a very small wavelength dependence and the population decays appear to be single exponential after the initial fast spectral diffusion contribution. However, we know there are two environments, ODs bound to water molecules and ODs bound to B−H's from the spectral decomposition in Figure 1 and the 2D-IR spectra discussed below. The conclusion is that the vibrational lifetime of an OD bound to a B−H is almost the same as that of an OD bound to water. If the time constants of a biexponential are similar enough, it becomes difficult to distinguish the two time constants in a fit: the data will be well described by a single exponential with a intermediate decay time. So the borohydride-associated water may have a slightly different lifetime than the water-associated water, but we cannot distinguish the two populations in the fit because the time scales are so similar.

The similarity between the OD vibrational lifetimes when OD is bound to water or to borohydride is unusual. Frequently, when water is bound to anions, the hydroxyl stretch vibrational lifetime changes significantly. Studies of the OD stretch in sodium bromide aqueous solutions show a combined water-associated and salt-associated population decay with a relaxation time constant of 6.7 ps.[67] A study of a wider range of halide salts saw the lifetime increase 3−6 times depending on ion.[84] However, a vibrationally excited hydroxyl hydrogen bonded to a halide anion cannot deposit vibrational energy into it. Borohydride is quite different. Like water itself, borohydride provides a collection of vibrational modes that can accept vibrational energy from the initially excited OD stretch. This availability of borohydride accepting modes may account for the similarity of the OD−water and OD−borohydride vibrational lifetimes.

The same type of pump−probe measurements were made on the B−H stretch of borohydride in a more dilute solution (1 M), which is also used for the 2D-IR experiments on the B−H stretch. The population relaxation data were taken over a range of wavelengths and are shown in Figure 5. The vibrational lifetime is independent of wavelength. The laser bandwidth was sufficient to pump the entire band, and thus a spectral diffusion short time decay is not observed. The black dashed curve is a single exponential fit. The B−H stretch lifetime is 2.9 ± 0.1 ps. Data were taken over a wide enough wavelength range that the side lobes of the main peak would contribute if they decayed as separate populations. No wavelength dependence was observed. The side lobes gain their oscillator strength through mixing with the light state, the triply degenerate B−H stretching mode. The mixing is sufficient to make the coupled system decay with a single lifetime.

DOI: 10.1021/jp512426y
J. Phys. Chem. B 2015, 119, 3546−3559

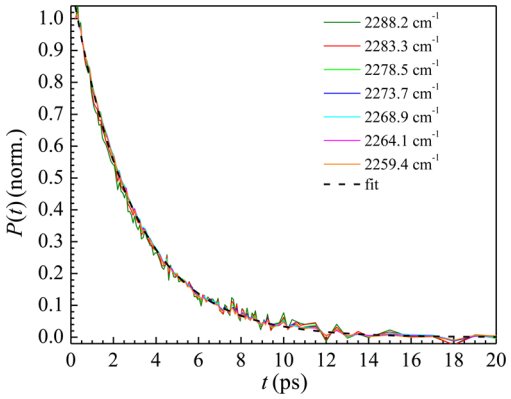

Figure 5. Normalized $P(t)$ for the B−H stretch of 1 M sodium borohydride in pH 14 water at various wavelengths and a single exponential fit (dashed black curve). There is no wavelength dependence of the 2.9 ± 0.1 ps vibrational lifetime.

C. Spectral Diffusion. 2D-IR vibrational echo experiments on both the O−D stretch of hydroxyls bound to borohydride in water and the B−H stretch of borohydride in water provide information on the systems' structural dynamics from the perspectives of water dihydrogen bonded to the anion and the anion itself. In vibrational echo experiments, three excitation pulses are crossed in the sample. A much weaker fourth pulse serves as a local oscillator (LO). The time between pulses 1 and 2 is the coherence time, τ; the time between pulses 2 and 3 is the population time, T_w. The third order nonlinear interaction of the three excitation pulses gives rise to a fourth pulse, the vibrational echo, at a time $\leq\tau$ after the third excitation pulse. The echo propagates in a unique direction because of wave vector matching. The LO is then spatially and temporally overlapped with the vibrational echo. This heterodyne detection amplifies the vibrational echo and provides phase information through the temporal interference between the LO and echo pulses. At a given T_w, data were collected by scanning τ, which causes the phase of the vibrational echo pulse to evolve in time relative to the temporally fixed LO pulse. The resulting temporal interferogram was frequency resolved and detected on the 32-element array, providing the vertical axis, ω_m, of the 2D-IR spectra. At each ω_m the interferogram is numerically Fourier transformed to give the horizontal axis, ω_τ, of the 2D-IR spectra.

The change in shape of the 2D-IR spectrum as a function of T_w is caused by spectral diffusion, which reports on the structural dynamics. Inhomogeneous broadening of both the O−D stretch spectrum (see Figure 1) and the B−H stretch spectrum (see Figure 2) gives rise to a range of transition frequencies. The liquid structure interacting with an individual molecular vibration determines the center frequency of its Lorentzian line that has a width from homogeneous broadening. The total absorption line is the collection of the individual molecules' Lorentzians with an essentially Gaussian distribution of center frequencies. Structural evolution of the medium causes the vibrational frequencies to change. Thus, as the liquid structure changes, the frequency of a particular molecule will change in time (spectral diffusion). At sufficiently long T_w, the vibrational probe will have sampled all liquid structures; hence all of the frequencies present in the inhomogeneously broadened FT-IR absorption spectrum will have been sampled as well.

In effect, the first and second pulses of the vibrational echo pulse sequence "label" the initial probe frequencies. Then during the waiting time, T_w, between pulse 2 and 3, the structure of the liquid evolves, causing the vibrational frequencies to shift. This period is ended by the arrival of the third pulse, which also stimulates the emission of the vibrational echo pulse. The echo contains information on the final frequencies of the vibrational oscillators. When T_w is short, the structure of the liquid is relatively unchanged from when the vibrations were first labeled, producing final frequencies that differ little from the starting frequencies. At longer T_w, the liquid structure has had more time to evolve, and the final frequencies are less correlated with the initial frequencies. The loss of correlation as T_w increases is manifested as a change in shape of the 2D-IR spectrum. At short T_w, the 2D spectrum is elongated along the diagonal (the slope = +1 line which bisects the vertical and horizontal frequency axes). As T_w increases and frequencies are less correlated, the shape of the spectrum becomes more symmetrical. If the population relaxation time is long enough to permit all of the environments to be sampled within the experimental time window, which is limited by the vibrational lifetime, the spectrum will become round. Thus, the structural dynamics of the liquid can be extracted from the change in shape of the 2D-IR spectra as a function of T_w.

The amplitudes and time scales of spectral diffusion are quantified by the frequency−frequency correlation function (FFCF). The FFCF is the joint probability that a vibrational oscillator with an initial frequency will have that same frequency at a later time, averaged over all of the initial frequencies in the inhomogeneous spectral distribution. The Center Line Slope (CLS) method[85,86] is used to extract the FFCF from the T_w dependence of the shape of the 2D-IR spectra.

The FFCF was modeled with the form

$$C(t) = \langle \delta\omega(t)\delta\omega(0)\rangle = \sum_i \Delta_i^2 \exp(-t/\tau_i) \tag{4}$$

where Δ_i and τ_i are the frequency fluctuation amplitude and time constant, respectively, of the i-th component. A component of the FFCF is motionally narrowed and a source of homogeneous broadening in the absorption line if $\tau\ \Delta < 1$. In this instance, it is not possible to determine Δ and τ separately. The motionally narrowed contribution to the absorption spectrum has a pure dephasing line width given by $\Gamma^* = \Delta^2\tau = 1/\pi T_2^*$, where T_2^* is the pure dephasing time. The total homogeneous dephasing time that is measured, T_2, also depends on the transition dipole orientational relaxation and vibrational lifetime and is given by

$$\frac{1}{T_2} = \frac{1}{T_2^*} + \frac{1}{2T_1} + \frac{1}{3T_{or}} \tag{5}$$

where T_1 and T_{or} are the vibrational lifetime and orientational relaxation time. The CLS has been previously shown to be mathematically equivalent to the normalized T_w-dependent portion of the FFCF.[85,86] Combining the T_w dependence from the CLS with the linear absorption spectrum of the vibrational probe enables the determination of the homogeneous contribution and the resulting full FFCF to be obtained.[85,86] The CLS decays have the same time constants as the FFCF and can be used to discuss the time scales of the dynamical processes in the sample. Computing the FFCF allows these processes to be assigned their respective contributions to the line width. FFCF parameters are given in Table 1.

DOI: 10.1021/jp512426y
J. Phys. Chem. B 2015, 119, 3546−3559

Table 1. FFCF Parameters

pH	vibration/sample	Γ (cm^{-1})	Δ_1 (cm^{-1})	τ_1 (ps)	Δ_2 (cm^{-1})	τ_2 (ps)
7	OD bound to H_2O[a]	76 ± 14	41 ± 8	0.4 ± 0.1	34 ± 11	1.7 ± 0.4
14	OD bound to H_2O	78 ± 4	45 ± 3	0.3 ± 0.1	38 ± 4	1.8 ± 0.4
14	OD bound to BH_4^-	42.3 ± 0.8	18.8 ± 0.5	0.3 ± 0.1	22.8 ± 1.3	2.2 ± 0.5
14	BH bound to H_2O	54.5 ± 0.3	10.1 ± 0.3	0.28 ± 0.06	5.3 ± 0.7	1.8 ± 0.5

[a]Numbers reproduced from ref 67.

The CLS decays for the O−D stretch of dilute HOD in water and in 1 M NaOH solution are shown in Figure 6. Data for the two samples are identical within experimental error. The blue line is a biexponential fit, with decay time constants of 0.3 ± 0.1 ps and 1.8 ± 0.1 ps. These are the same decay times, within experimental error, that have been obtained previously in studies of water.[67] The spectral diffusion of the OD stretch in the two liquids is identical within experimental error. Water is 55 M in H_2O molecules, which means it is 110 M in hydroxyls. Therefore, only a small fraction of the ODs will be directly associated with the hydroxides. In the results shown in Figure 6, we are looking at the total solution, not the ODs specifically interacting with the hydroxides. The important point is that for the studies involving borohydride, which require the 1 M NaOH to slow the borohydride chemical decomposition, the medium has virtually the same dynamics as water with little impact from the NaOH.

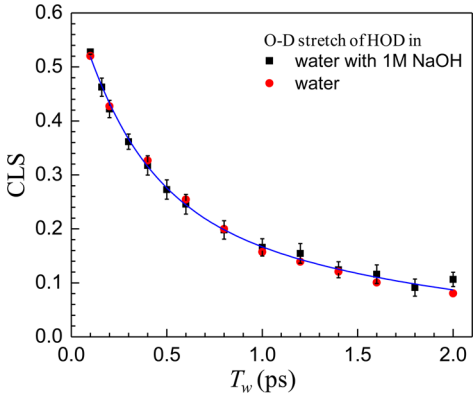

Figure 6. Spectral diffusion represented by the CLS experimental observable of the OD stretch of HOD in 1 M NaOH (pH 14) solution (black squares) and in pure water (red circles). The data points are the average of six measurements, and error bars are the standard error. The data in the two solutions are indistinguishable. The blue curve is a biexponential fit to both data sets.

Extracting the CLS from the 2D-IR spectra for only the O−D's that are dihydrogen bonded to borohydrides requires careful processing of the data. As can be seen in Figure 1, the absorption spectrum of the O−D's bound to borohydrides (green curve) is blue-shifted but still subsumed in the total spectrum that is dominated by O−D's hydrogen bonded to water molecules. Nonetheless, it is clear from Figure 1 that there are two distinct populations in solution. The 2D-IR spectra have the appearance of two overlapping bands (Figure 7B) with centers that approximately correspond to the peaks of the blue curve (O−D bound to water) and the green curve (O−D bound to borohydride) in Figure 1. However, the two 2D-IR bands are not sufficiently separated that CLS analysis can be performed on them individually. For overlapping spectra that are essentially on top of each other, the two-component

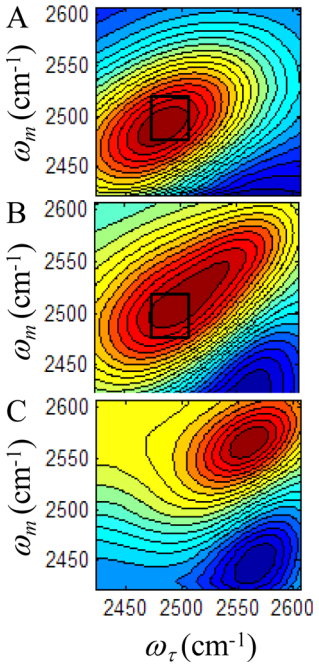

Figure 7. 2D-IR spectra of the OD stretch of HOD at short T_w = 0.2 ps. (A) In 1 M NaOH solution. (B) In 1 M NaOH with 8:1 H_2O/$NaBH_4$. The squares in A and B are in regions of the spectra where there is essentially no contribution from ODs bound to borohydride (see green curve in Figure 1). The two spectra are matched in amplitude in the boxed regions, and the spectra are subtracted. (C) The subtracted spectrum, which is the 2D-IR spectrum of ODs bound to borohydride.

CLS method can be applied.[87] However, here the two bands are too separated to apply that method, but not separated enough to treat them as distinct spectra.

A subtraction method was used to extract the 2D data for ODs bound to borohydride so that the CLS can be obtained. The method is somewhat similar to that applied by Roberts et al. to subtract out a large diagonal band to see off-diagonal bands,[76] but they were not trying to obtain line shapes from a band masked by another band. Figure 7A and B show 2D-IR data taken at 200 fs on the OD stretch of HOD in the solution of HOD/water/NaOH without and with $NaBH_4^-$, respectively. The spectrum in Figure 7B (with borohydride) has significant amplitude in the region around 2600 cm^{-1}, while the spectrum in Figure 7A (no borohydride) has little amplitude in this region. This difference is consistent with the decomposition of the absorption spectrum shown in Figure 1. To obtain the desired time dependent 2D spectra of the ODs bound to borohydride, at each T_w the spectrum like that in Figure 7A is subtracted from the spectrum like that in 7B. However, it is necessary to have the correct amplitude of the borohydride-free spectrum when it is subtracted from the spectrum with borohydride. This is accomplished by selecting a region of the

DOI: 10.1021/jp512426y
J. Phys. Chem. B 2015, 119, 3546−3559

2D-IR spectra in which there is essentially no contribution from ODs bound to borohydrides. These are the black rectangles in Figure 7A and B. The spectrum in Figure 7A was scaled until the difference between the two spectra in this region was minimized. Then the subtraction was performed. Note that we carried out the same procedure using different choices of the region on the red side of the spectra, and the results were the same. Figure 7C shows the results of the subtraction, which is the 2D-IR spectrum of the ODs bound to borohydride. It is important to mention that the CLS method uses the central region of the 2D spectrum to extract the dynamics. Therefore, small errors in subtraction, which can affect the low amplitude contours in the resulting spectrum, will not affect the analysis of the dynamics. Spectra at a series of T_w's both before and after subtraction are given in the Supporting Information.

Figure 8 shows CLS data for the O−Ds bound to borohydride obtained using the subtraction method (green squares) and a biexponential fit to the data (green curve). Also shown for comparison are the data from Figure 6 that are the CLS data for O−D's in water (red squares) and in water with NaOH (black squares). It is clear from the plot that the spectral diffusion of the O−D stretch of HOD for O−D's dihydrogen bonded to B−H's is very similar to that of O−D's bound to O−H's of water. The CLS decay constants for O−D's bound to borohydride are 0.3 ± 0.1 and 2.2 ± 0.5 ps. The decay constants for O−D's bound to the O−H's of water are 0.4 ± 0.1 and 1.7 ± 0.5 ps.[67] The full FFCF parameters are given in Table 1. While the data for the OD/BH shown in Figure 8 are somewhat slower than the other data, the decay times are within the error bars of the fits. Additionally, even though the curves look different, part of this is caused by a difference in the relative amplitudes of the decays rather than a substantial difference in the time constants. The ODs associated with the borohydrides have a narrowed and shifted spectrum (see Figure 1, green curve). Differences in the spectral width and shape will result in different relative amplitudes in the CLS, but the time constants will remain the same if the dynamics are the same. The clear message is that O−D's bound to borohydride and O−D's bound to water hydroxyls experience little difference in their structural dynamics.

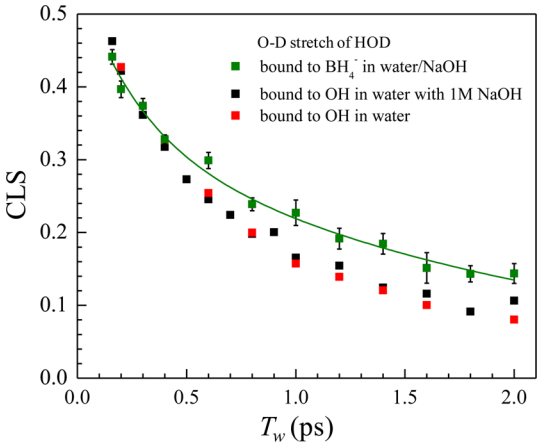

Figure 8. Spectral diffusion CLS decay of the ODs dihydrogen bonded to the B−H's of borohydride (green squares) and the biexponential fit (green curve). The data points are the average of four measurements, and error bars are the standard error. The data from Figure 6 are displayed for comparison. The spectral diffusion of ODs dihydrogen bonded to the B−H's of borohydride is almost the same as the spectral diffusion in the solutions without borohydride. The fits (Figures 6 and 8) yield time constants that are the same within the error bars.

Detailed comparisons of 2D-IR vibrational echo experiments and molecular dynamics (MD) simulations of the OD stretch of HOD in water showed that the fast component of the spectral diffusion is associated with very local hydrogen bond motions, in particular hydrogen bond length fluctuations.[47,56] The slow component is caused by the randomization of the hydrogen bond network that involves hydrogen bond breaking and formation. Assuming that the fast and slow components of the spectral diffusion of ODs dihydrogen bonded to borohydride involve the same physical processes as ODs bound to water, then the local hydrogen bond length fluctuations may be slightly faster for the OD−HB bond, but the error bars of the measurements overlap. The slow component of the spectral diffusion of the OD stretch of HOD in water is caused by the concerted hydrogen bond rearrangement of the water molecules that are hydrogen bonded to the HOD and surrounding water molecules. The slow component of the spectral diffusion for OD-HB is slightly slower, but again within the error bars of ODs bound to water. The results suggest that the spectral diffusion of the ODs bound to borohydride is caused by the hydrogen bond dynamics of the surrounding water molecules, and the water dynamics in the vicinity of the borohydride anion are not significantly affected by the presence of the anion.

Further information can be obtained by considering the spectral diffusion of the borohydride asymmetric stretching mode with the B−H's hydrogen bonded to water molecules. Figure 9 displays the CLS data for the B−H stretch (circles) and a biexponential fit to the data (solid curve). The full FFCF parameters are given in Table 1. The spectral diffusion decay time constants are 0.28 ± 0.06 and 1.8 ± 0.5. These decays are the same as those found for the OD stretch of HOD in bulk water and the OD stretch of HOD bound to borohydride within experimental error, although the OD/borohydride spectral diffusion appears to be somewhat slower as can be seen in Figure 8. One major difference in the B−H dynamics is that there is a much larger homogeneous component relative to the inhomogeneous component. This can be seen clearly from

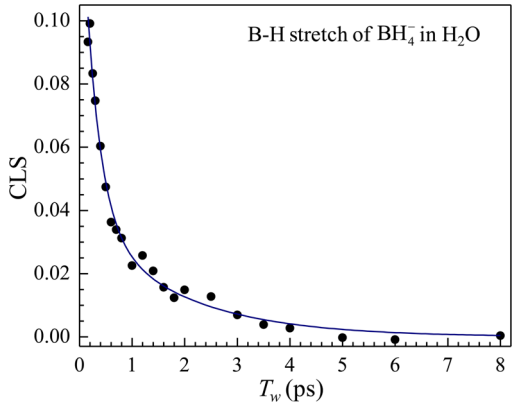

Figure 9. Spectral diffusion CLS decay data (black circles) of the B−H stretch of 1 M sodium borohydride in pH 14 water. Note the large initial difference from 1, which indicates a substantial homogeneous component. The blue curve is the biexponential fit to the data, which yields decay time constants of 0.3 and 1.8 ps. These time constants are the same within error as the time constants for the OD stretch of HOD in pure water, 0.4 and 1.7 ps.

DOI: 10.1021/jp512426y
J. Phys. Chem. B 2015, 119, 3546−3559

the CLS plots in Figures 8 and 9. The T_w = 0 values from extrapolation of the fit curves for the OD stretch in water, water/NaOH, and bound to borohydride are all ~0.6 (Figure 8). In contrast, the T_w = 0 value for the B−H CLS curve (Figure 9) is ~0.15. The difference of the T_w = 0 value from 1 is directly related to the fraction of the absorption line width that is the result of homogeneous broadening. The homogeneous broadening from pure dephasing is caused by ultrafast fluctuations that produce a motionally narrowed Lorentzian contribution to the absorption spectrum. The B−H stretch homogeneous component will be discussed further below.

The fact that the B−H stretch spectral diffusion is almost identical to that of the O−D stretch of HOD in bulk water and the OD stretch bound to borohydride is highly suggestive. The sample used for these measurements was a 1 M borohydride solution; so, there are no issues of ion pairing or incomplete solvation as the sample is relatively dilute, 55 water molecules per borohydride. The borohydride dynamics are presumably caused by dihydrogen bonded water molecules and the surrounding water. Borohydride is experiencing the same structural fluctuations as its solvating water. Borohydride is tetrahedral. It has a calculated radius for the isolated anion of ~1.9 Å compared to water's ~1.35 Å. Therefore, borohydride is larger than water. However, the tetrahedral arrangement of the B−H bonds may permit water to dihydrogen bond to it without greatly perturbing the nominally tetrahedral hydrogen bonding structure of the surrounding water. The results suggest that the hydrogen bonding does not enforce strained structures on the dihydrogen bound waters but rather can allow the water to coordinate at angles native to the bulk water structure.

D. Anisotropy. From the same pump probe data used to obtain the vibrational lifetimes discussed above, the anisotropy can be extracted. The anisotropy is equal to the transition dipole orientational correlation function (second Legendre polynomial correlation function, $C_2(t)$) scaled by 0.4. It has the form

$$r(t) = \frac{S_{\parallel}(t) - S_{\perp}(t)}{S_{\parallel}(t) + 2S_{\perp}(t)} = 0.4C_2(t) \quad (6)$$

The anisotropies were obtained for both the B−H and O−D stretches in pH 14 water. The O−D anisotropy decay was also collected for the 1 M NaOH solution and pure HOD in H_2O for comparison.

First we consider the anisotropy of the triply degenerate asymmetric stretch of borohydride. Data are shown in Figure 10. The main body of the figure shows the data (circles) and a single exponential fit to the data (solid curve) on the full vertical scale where the maximum initial anisotropy can be as great as 0.4 (see eq 4). The inset shows the data on a greatly expanded vertical scale. By 200 fs, the time at which meaningful data can start to be collected, the anisotropy is already at ~0.065. Fitting the curve from this point on gives a decay time constant of 200 fs. In less than a picosecond, the anisotropy has decayed to zero. Most of the anisotropy decay occurs on a time scale much faster than this 200 fs decay. The ultrafast anisotropy decay can be compared to a Debey−Stokes−Einstein (DSE) equation[88] calculation of the orientational relaxation time of borohydride in the water/NaOH solution, which has a viscosity ~30% greater than that of water. This calculation gives the orientational relaxation time of ~8 ps. The DSE decay is for physical orientational relaxation of the borohydride anion, taking it to be spherical with stick boundary

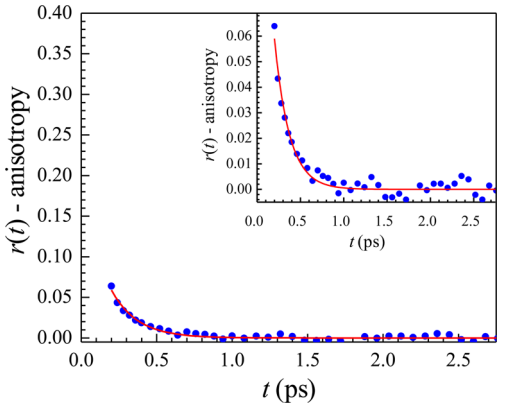

Figure 10. Anisotropy decay, $r(t)$, for the B−H stretch of 1 M sodium borohydride in pH 14 water (blue circles) and an exponential fit (red curve). The inset is an expanded view of the data. The anisotropy decay is wavelength independent. Note by the beginning of the measurement at 200 fs there is almost no anisotropy and the remaining anisotropy decays with a 200 fs time constant. The anisotropy decay is not caused by reorientation of the molecule. See text.

conditions. Although there will be some error in calculating the orientational relaxation time with the DSE equation, the results show that the ultrafast loss of the anisotropy cannot occur through physical reorientation of the molecule.

The anisotropy decay of the asymmetric B−H stretch of BH_4^- is not caused by normal molecular reorientation. The B−H stretch is triply degenerate. The excitation pulse projects out a superposition of the three modes that results in the initially excited transition dipole being along the pump pulse electric field, in contrast to the usual initial cosine squared distribution of dipole directions.[89] Structural fluctuations of the environment that cause the relative amplitudes of the three components of the initial superposition to change produce a change in the direction of the transition dipole without physical reorientation of the molecule.[89] Therefore, the anisotropy decay does not provide the type of information that normal orientational relaxation measurements do and cannot be interpreted in terms of shape factors, hydrodynamic boundary conditions, or friction coefficients.

The vast majority of the anisotropy decay is occurring much faster than the very low amplitude very fast 200 fs decay. This ultrafast anisotropy decay is the result of the evolution of the initial superposition of degenerate modes. Consequently, on times that are long compared to a few hundred femtoseconds, the direction of the transition dipole has randomized. The structural fluctuations that contribute to the dynamic B−H stretch line shape occur on three time scales (see Table 1). There are the ultrafast fluctuations that are associated with the pure dephasing contribution to the homogeneous line and the 0.28 and 1.8 ps spectral diffusion components. It is likely that the ultrafast pure dephasing fluctuations are responsible for inducing the bulk of the dipole direction randomization, while the final complete randomization is caused by the same fluctuations that give rise to the fast component of the spectral diffusion. On the time scale of the slow component of the spectral diffusion, the transition dipole direction has completely randomized.

These results show that there is a portion of the inhomogeneous line that is sampled on a time scale that is much longer than the randomization of the transition dipole

DOI: 10.1021/jp512426y
J. Phys. Chem. B 2015, 119, 3546−3559

direction. Because the transition dipole direction randomizes on a time scale much faster than the slow component of the spectral diffusion, the inhomogeneous frequency sampling associated with the slow component cannot depend on the direction of the transition dipole. Therefore, the slow component of the spectral diffusion is not caused by fluctuations of the electric field projected along the vibrational transition dipole direction, a mechanism that has been invoked in a number of spectral diffusion studies of other types of systems.[90−93] These considerations suggest that the 1.8 ps component of the spectral diffusion is associated with evolution of specific hydrogen bonding configurations of water directly bound to the B−H's and possibly the water molecules in the next solvation shell. Changes in water configurations modify the intermolecular interactions with the B−H's, producing changes in the B−H internuclear potential, and therefore the vibrational transition frequency.

Figure 11 displays orientational anisotropy decays for the O−D stretch of HOD in water (blue), water with 1 M NaOH (red), and water with 1 M NaOH and $NaBH_4$ with 8 water molecules per borohydride (green). The dashed curves are single exponential fits to the data. In these data, the difference between 0.4 and the initial values of the curves at t = 0, obtained by extrapolating the curves to t = 0, is caused by inertial motion of the HOD.[94] The data were taken as a function of wavelength, and within experimental error, there is no wavelength dependence. The water (blue) and the water/NaOH (red) curves shown were for data taken at the peak of the O−D stretch spectra (see Figure 3), while the data shown for the solution with borohydride was taken near the peak of the green curve in Figure 1, that is, around the maximum of the spectrum from ODs bound to borohydride. The HOD in water data requires the standard heat subtraction to obtain the anisotropy.[54,79] The extraction of the OD anisotropy decay for the samples with OH^- requires a different procedure. The water solution of 1 M NaOH with no HOD has very broad background absorption which includes the spectral region of the O−D stretch.[78] Relaxation then produces heat in the sample that grows in and produces a pump−probe signal. The initial portion of the heating signal displays an anisotropy, which has been discussed by Bakker and co-workers.[77,78] To obtain the anisotropy decays of the O−D stretch caused by orientational relaxation of HOD, the $S_{\|}$ and $S_{\perp}$ were measured on samples with no HOD, and the contributions from the "solvent" were removed from the $S_{\|}$ and $S_{\perp}$ data taken on the samples with HOD. The data shown in Figure 11 have the solvent anisotropy and heating contributions removed.

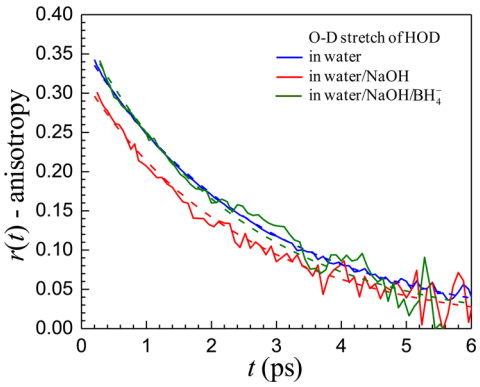

Figure 11. Anisotropy decay of the OD stretch of HOD in pure water (blue solid curve), in 1 M NaOH solution (red solid curve), and in 1 M NaOH and 8:1 $H_2O/NaBH_4$ (green solid curve). The corresponding dashed curves are single exponential fits to the data. The orientational relaxation time constants are the same for all three samples within experimental error.

The HOD in pure water anisotropy decays as a single exponential with a time constant of 2.6 ± 0.1 ps (Figure 11, data - blue solid curve, fit - blue dashed curve).[94] The addition of 1 M NaOH has little influence on the time scale of the HOD anisotropy decay. The data are fit with a single exponential function (data, red solid curves; fit, red dashed curve). The decay constant is 2.5 ± 0.1 ps, which is the same as pure water within experimental error. While the anisotropy decay times for HOD in water/NaOH solution showed no wavelength dependence within experimental error, the initial amplitude does change with wavelength. The difference between 0.4 and the t = 0 value becomes larger as the measurements are made further to the blue; that is, the magnitude of the initial inertial orientational relaxation increases. This behavior has been discussed in detail for pure bulk water and was attributed to weaker hydrogen bonding as the frequency shifts to blue.[94] The weaker hydrogen bonds enable a larger inertial angular cone to be sampled. The fact that the observed orientational relaxation of HOD in water with 1 M NaOH is essentially the same as that found in pure water is not surprising. It has been suggested that ∼4−5 water molecules are associated with each hydroxide.[78,95] These water molecules may have orientational relaxation that is distinct from pure water. However, the anisotropy signal arises from all HOD molecules, bulk-like and hydroxide associated. Because the vast majority of the water is not affected by the hydroxide, the measurements yield an anisotropy decay that is essentially that of pure water.

The solid green curve is the data for the sample with borohydride. The fit is the dashed green curve. While the signal-to-noise ratio is not as good for these data as for the other decays, it is clear that the orientational anisotropy decay is almost identical to that found for pure water. Again, the data are not wavelength dependent within experimental error. The fit yields 2.4 ± 0.2 ps. Therefore, the orientational relaxation of HOD in all three samples is the same within experimental error.

The 2D-IR spectra at longer times (∼2 ps) may show evidence of chemical exchange between O−D's dihydrogen bonded to borohydride and O−D's hydrogen bonded to water molecules. Chemical exchange would be manifested through the growth of off-diagonal peaks as T_w is increased.[4,96] However, because of the method used to extract the 2D spectra for the O−D's bound to borohydride, the possible appearance of off-diagonal peaks is not definitive. The peaks would be caused by ODs that are initially bound to borohydride that break the dihydrogen bond and make a hydrogen bond with water, and vice versa. Chemical exchange was observed previously for the system of sodium tetrafluoroborate in water.[4] The switching of ODs of HOD from being bound to the tetrafluoroborate anion to being bound to water has a time constant of 7 ps in the tetrafluoroborate system.[4] The OD stretching mode of ODs bound to BF_4^-'s occurs as a distinct peak that is relatively well separated from the OD/water band, which makes the off-diagonal peaks relatively easy to observe. In addition, the lifetime of ODs bound to BF_4^-'s is significantly longer than the lifetime of ODs bound to BH_4^-, which makes it possible to observe slower exchange processes. Chemical exchange of HOD between an anion and water is accompanied by a change in dipole direction, i.e., orientation

DOI: 10.1021/jp512426y
J. Phys. Chem. B 2015, 119, 3546−3559

relaxation.[3]The possible appearance of off-diagonal peaks in the borohydride sample occurs on the correct time scale of the orientational relaxation, but again, the data are not definitive.

The combination of all of the results for the dynamics of dihydrogen bonded water to borohydride is surprising. The spectral diffusion of the O−D stretch of HODs that are dihydrogen bonded to borohydride is only slightly slower than HOD in pure bulk water, but the error bars of the measurements overlap. The spectral diffusion of the B−H stretch of borohydride dihydrogen bonded to water (1 M solution) is the same as that of the O−D stretch of pure bulk water. Furthermore, the orientational relaxation of HOD in the borohydride solution (8 water molecules per borohydride) is essentially identical to HOD in pure bulk water.

Similar experiments have been conducted on solutions of NaBr.[67] Bromide has about the same volume as borohydride. Measurements of the HOD orientational relaxation time scale in the NaBr solution with 8 water molecules per bromide anion (which is the same concentration as the $NaBH_4$ solution) yield 6.7 ps in contrast to 2.4 ps for the borohydride solution. The high concentration of NaBr in water slows the orientational relaxation of water significantly. Recall that the $NaBH_4$ solution had approximately the same spectral diffusion time constants as bulk water. In the same concentration NaBr solution (8 water molecules per ion pair), the biexponential O−D stretch CLS decay time constants (spectral diffusion) are 0.63 ± 0.09 ps and 4.8 ± 0.6 ps, which are significantly slower. In the 2D-IR experiments on the borohydride solution, we were able to measure the spectral diffusion of OD bound to borohydride, eliminating the contribution from OD bound to other water molecules. In the NaBr solution this separation was not possible because the spectra of OD in water and OD in the NaBr solution overlap too much. Therefore, the spectral diffusion measured for NaBr is a combination of ODs bound to Br^- and ODs bound to water. It is likely that the spectral diffusion of ODs directly bound to Br^- is even slower than the measured numbers obtained on the total solution.

In both the $NaBH_4$ and NaBr solutions there are 8 water molecules per ion pair. Perhaps a better way to think about this is that there are 16 water hydroxyls per anion. Br^- is solvated by 6 water molecules in aqueous solution, which means that 6 hydroxyls are making hydrogen bonds to the bromide in a nominally octahedral arrangement.[14,97] Thus, the waters solvating Br^- will not have the tetrahedral arrangement of the hydrogen bonding network in pure water. The octahedral structure will not match well with the normal tetrahedral hydrogen bonding network of water. It is reasonable to assume, and ref 46 suggests, that water will make 4 dihydrogen bonds to the B−H's of borohydride in a tetrahedral geometry. Borohydride is bigger than water, so the tetrahedron of dihydrogen bonded waters around the borohydride will be expanded relative to the tetrahedral hydrogen bonds in bulk water. For two borohydrides there are 32 hydroxyls, of which 8 will be dihydrogen bonded to the borohydrides. The rest of the water hydroxyls may form a bridging network between the borohydrides, and the tetrahedral borohydride geometry may make it possible for the bridging networks to have relatively normal water hydrogen bond arrangements. This postulated relatively normal hydrogen bond arrangement gives rise to the observed hydrogen bond dynamics that are virtually the same as those of bulk water. In contrast, octahedral arrangement around bromide might produce very distorted water hydrogen bond structures bridging the anions. In bulk water, the slowest component of the spectral diffusion is associated with hydrogen bond structure randomization,[47,56] which occurs through a concerted jump reorientation mechanism.[98] A highly distorted hydrogen bond geometry in the concentrated bromide solution could inhibit the jump reorientation and produce slower orientational relaxation and spectral diffusion compared to pure water. In contrast, a tetrahedral geometry in the concentrated borohydride solution might permit normal jump reorientations and, therefore, orientational relaxation and spectral diffusion indistinguishable from pure water.

IV. CONCLUDING REMARKS

We have examined the dynamics of dihydrogen bonds between borohydride and water using ultrafast 2D-IR vibrational echo spectroscopy and polarization selective IR pump−probe experiments. In the experiments we were able to measure the dynamics from the perspectives of the water hydroxyls bound to borohydride and the B−H's of the borohydride anion bound to water. Structural evolution of the systems is reflected in spectral diffusion measured with 2D-IR. Spectral diffusion of hydroxyls that were bound to borohydride was made possible by a new data analysis procedure that removed the contributions to the data from water hydroxyls bound to other water molecules. The spectral diffusion of the B−H stretch could be measured directly, as the absorption band is well separated from strong water absorptions. In addition, orientational relaxation of water was measured with the pump−probe experiments in the concentrated $NaBH_4$ solutions.

The remarkable results are that the B−H stretching mode and the hydroxyls (OD stretch of HOD) bound to the B−H's show virtually identical spectral diffusion dynamics that are in turn identical to those of the OD stretch of HOD in pure bulk water within relatively small error bars. In bulk water, detailed comparisons of molecular dynamics simulations to 2D-IR data have shown that spectral diffusion, which occurs on two time scales, is associated with hydrogen bond dynamics.[47,56] Ultrafast dynamics, ∼0.4 ps, are caused by hydrogen bond length fluctuations, while slower dynamics, ∼1.7 ps, are caused by randomization of the hydrogen bonding network. Although the hydroxyls and BHs form dihydrogen bonds, the ultrafast fluctuations observed for both the B−H stretch and O−D stretch, which are presumably length fluctuations as in pure water, occur with the same time constants as pure water within error. In addition, the orientational relaxation of HOD in the concentrated $NaBH_4$ solution (8 water molecules per ion pair) is the same as it is in pure water within a small experimental error. The fact that the dynamics in borohydride solution is the same as in pure water is in contrast to results on other concentrated salt solutions, where generally both the spectral diffusion and the orientational relaxation are considerably slower.[1,67]

The results presented here are a detailed examination of the dynamics and strength of dihydrogen bonds to water. In Figure 1, the decomposed spectrum (green curve) shows that a water hydroxyl dihydrogen bonded to B−H makes a weaker hydrogen bond than a water hydroxyl hydrogen bonded to another water molecule. The average dihydrogen bond falls within the broad range of strengths of water hydrogen bonds, but is on the weak side of the distribution. As described above, the dihydrogen bond, although somewhat weaker than the average water hydrogen bond, has dynamics that are virtually identical to those of water hydrogen bonds. Therefore, at least for the borohydride anion dihydrogen bonding in water, the

DOI: 10.1021/jp512426y
J. Phys. Chem. B 2015, 119, 3546−3559

nature of these dihydrogen bonds is very similar to that of water hydrogen bonds.

■ ASSOCIATED CONTENT

Supporting Information

Additional FT-IR spectra and 2D IR spectra. FT-IR spectra showing data prior to subtraction of background spectra. Addition 2D IR spectra showing addition T_w's. This material is available free of charge via the Internet at http://pubs.acs.org.

■ AUTHOR INFORMATION

Corresponding Author

*E-mail: fayer@stanford.edu.

Notes

The authors declare no competing financial interest.

■ ACKNOWLEDGMENTS

We would like to thank Professor James (Ned) Jackson, Department of Chemistry, Michigan State University for many very useful discussions about this work. This work was funded by the Division of Chemical Sciences, Geosciences, and Biosciences, Office of Basic Energy Sciences of the U.S. Department of Energy through Grant No. DE-FG03-84ER13251. P.L.K. acknowledges support from an Abbott Laboratories Stanford Graduate Fellowship.

■ REFERENCES

(1) Giammanco, C. H.; Wong, D. B.; Fayer, M. D. Water Dynamics in Divalent and Monovalent Concentrated Salt Solutions. *J. Phys. Chem. B* **2012**, *116*, 13781.

(2) Bakker, H. J.; Kropman, M. F.; Omata, Y.; Woutersen, S. Hydrogen-Bond Dynamics of Water in Ionic Solutions. *Phys. Scr.* **2004**, *69*, C14.

(3) Ji, M.; Gaffney, K. J. Orientational Relaxation Dynamics in Aqueous Ionic Solution: Polarization-Selective Two-Dimensional Infrared Study of Angular Jump-Exchange Dynamics in Aqueous 6 M $NaClO_4$. *J. Chem. Phys.* **2011**, *134*, 044516.

(4) Moilanen, D. E.; Wong, D.; Rosenfeld, D. E.; Fenn, E. E.; Fayer, M. D. Ion-Water Hydrogen-Bond Switching Observed with 2D-IR Vibrational Echo Chemical Exchange Spectroscopy. *Proc. Natl. Acad. Sci. U.S.A.* **2009**, *106*, 375.

(5) Pines, E.; Huppert, D.; Agmon, N. Geminate Recombination in Excited-State Proton-Transfer Reactions: Numerical Solution of the Debye−Smoluchowski Equation with Backreaction and Comparison with Experimental Results. *J. Chem. Phys.* **1988**, *88*, 5620.

(6) Woutersen, S.; Bakker, H. Ultrafast Vibrational and Structural Dynamics of the Proton in Liquid Water. *Phys. Rev. Lett.* **2006**, *96*, 138305.

(7) Moilanen, D. E.; Piletic, I. R.; Fayer, M. D. Water Dynamics in Nafion Fuel Cell Membranes: The Effects of Confinement and Structural Changes on the Hydrogen Bonding Network. *J. Phys. Chem. C* **2007**, *111*, 8884.

(8) Spry, D. B.; Goun, A.; Glusac, K.; Moilanen, D. E.; Fayer, M. D. Proton Transport and the Water Environment in Nafion Fuel Cell Membranes and AOTReverse Micelles. *J. Am. Chem. Soc.* **2007**, *129*, 8122.

(9) Saenger, W. *Principles of Nucleic Acid Structure*; Springer-Verlag: New York, 1984

(10) Fersht, A. *Enzyme Structure and Mechanism*, 2nd ed.; W.H. Freeman: New York, 1985.

(11) Jeffrey, G.; Saenger, W. *Hydrogen Bonding in Biological Structures*; Springer-Verlag: New York, 1991.

(12) Daggett, V.; Fersht, A. The Present View of the Mechanism of Protein Folding. *Nat. Rev. Mol. Cell Biol.* **2003**, *4*, 497.

(13) Lin, Y. S.; Auer, B. M.; Skinner, J. L. Water Structure, Dynamics, and Vibrational Spectroscopy in Sodium Bromide Solutions. *J. Chem. Phys.* **2009**, *131*, 144511.

(14) Raugei, S.; Klein, M. L. An Ab Initio Study of Water Molecules in the Bromide Ion Solvation Shell. *J. Chem. Phys.* **2002**, *116*, 196.

(15) Smith, J. D.; Saykally, R. J.; Geissler, P. L. The Effect of Dissolved Halide Anions on Hydrogen Bonding in Liquid Water. *J. Am. Chem. Soc.* **2007**, *129*, 13847.

(16) Shimizu, A.; Taniguchi, Y. NMR Studies of Reorientational Motion of Hydrated D_2O Molecules of Halide Ions (F^-, Cl^-, Br^-, and I^-) in Dilute Aqueous Solutions. *Bull. Chem. Soc. Jpn.* **1991**, *64*, 1613.

(17) Omta, A. W.; Kropman, M. F.; Woutersen, S.; Bakker, H. J. Influence of Ions on the Hydrogen-Bond Structure in Liquid Water. *J. Chem. Phys.* **2003**, *119*, 12457.

(18) Tielrooij, K. J.; van der Post, S. T.; Hunger, J.; Bonn, M.; Bakker, H. J. Anisotropic Water Reorientation around Ions. *J. Phys. Chem. B* **2011**, *115*, 12638.

(19) Fayer, M. D.; Moilanen, D. E.; Wong, D.; Rosenfeld, D. E.; Fenn, E. E.; Park, S. Water Dynamics in Salt Solutions Studied with Ultrafast Two-Dimensional Infrared (2D-IR) Vibrational Echo Spectroscopy. *Acc. Chem. Res.* **2009**, *42*, 1210.

(20) Brown, M. P.; Heseltine, R. W. Co-ordinated BH_3 as a Proton Acceptor Group in Hydrogen Bonding. *Chem. Commun.* **1968**, 1551.

(21) Brown, M. P.; Heseltine, R. W.; Smith, P. A.; Walker, P. J. An Infrared Study of Co-ordinated BH_3 and BH_2 Groups as Proton Acceptors in Hydrogen Bonding. *J. Chem. Soc. A* **1970**, 410.

(22) Burg, A. B. Enhancement of P−H Bonding in a Phosphine Monoborane. *Inorg. Chem.* **1964**, *3*, 1325.

(23) Zachariasen, W. H.; Mooney, R. C. L. The Structure of the Hypophosphite Group as Determined from the Crystal Lattice of Ammonium Hypophosphite. *J. Chem. Phys.* **1934**, *2*, 34.

(24) Brown, M. P.; Walker, P. J. Hydrogen Bonds between Co-ordinated BH_3 and BH_2 Groups and OH Groups. Thermodynamics of Formation by Infrared Spectroscopy. *Spectrochim. Acta, Part A* **1974**, *30*, 1125.

(25) Crabtree, R. H.; Siegbahn, P. E. M.; Eisenstein, O.; Rheingold, A. L.; Koetzle, T. F. A New Intermolecular Interaction: Unconventional Hydrogen Bonds with Element−Hydride Bonds as Proton Acceptor. *Acc. Chem. Res.* **1996**, *29*, 348.

(26) Popelier, P. L. A. Characterization of a Dihydrogen Bond on the Basis of the Electron Density. *J. Phys. Chem. A* **1998**, *102*, 1873.

(27) Epstein, L. M.; Shubina, E. S.; Bakhmutova, E. V.; Saitkulova, L. N.; Bakhmutov, V. I.; Chistyakov, A. L.; Stankevich, I. V. Unusual Hydrogen Bonds with a Hydride Atom in Boron Hydrides Acting as Proton Acceptor. Spectroscopic and Theoretical Studies. *Inorg. Chem.* **1998**, *37*, 3013.

(28) Shubina, E. S.; Bakhmutova, E. V.; Saitkulova, L. N.; Epstein, L. M. Intermolecular Hydrogen Bonds BH···HX in Solution. *Mendeleev Commun.* **1997**, *7*, 83.

(29) Shubina, E. S.; Belkova, N. V.; Bakhmutova, E. V.; Saitkulova, L. N.; Ionidis, A. V.; Epstein, L. M. Problems of Unusual Hydrogen Bonds between Proton Donors and Transition Metal Hydrides and Borohydrides. *Russ. Chem. Bull.* **1998**, *47*, 817.

(30) Lee, J. C., Jr.; Peris, E.; Rheingold, A. L.; Crabtree, R. H. An Unusual Type of H−H Interaction: Ir−H−H−O and Ir−H−H−N Hydrogen Bonding and Its Involvement in Sigma-Bond Metathesis. *J. Am. Chem. Soc.* **1994**, *116*, 11014.

(31) Lough, A. J.; Park, S.; Ramachandran, R.; Morris, R. H. Switching on and Off a New Intramolecular Hydrogen−Hydrogen Interaction and the Heterolytic Splitting of Dihydrogen. Crystal and Molecular Structure of $[Ir\{H(SC_5H_4NH)\}_2(PCy_3)_2]BF_4{\cdot}2.7CH_2Cl_2$. *J. Am. Chem. Soc.* **1994**, *116*, 8356.

(32) Belkova, N. V.; Shubina, E. S.; Ionidis, A. V.; Epstein, L. M.; Jacobsen, H.; Messmer, A.; Berke, H. Intermolecular Hydrogen Bonding of $ReH_2(CO)(NO)L_2$ Hydrides with Perfluoro-*tert*-Butyl Alcohol. Competition between M−H···H−OR and M−NO···H−OR Interactions. *Inorg. Chem.* **1997**, *36*, 1522.

(33) Shubina, E. S.; Belkova, N. V.; Krylov, A. N.; Vorontsov, E. V.; Epstein, L. M.; Gusev, D. G.; Niedermann, M.; Berke, H.

DOI: 10.1021/jp512426y
J. Phys. Chem. B 2015, 119, 3546−3559

Spectroscopic Evidence for Intermolecular M−H···H−OR Hydrogen Bonding: Interaction of $WH(CO)_2(NO)L_2$ Hydrides with Acidic Alcohols. *J. Am. Chem. Soc.* **1996**, *118*, 1105.
(34) Yu, Z.; Wittbrodt, J. M.; Xia, A.; Heeg, M. J.; Schlegel, H. B.; Winter, C. H. Hydrogen and Dihydrogen Bonding as Important Features of the Reactivity of the Bridging Hydride in Pyrazolate-Bridged Dialuminum Complexes. *Organometallics* **2001**, *20*, 4301.
(35) Belkova, N. V.; Shubina, E. S.; Epstein, L. M. Diverse World of Unconventional Hydrogen Bonds. *Acc. Chem. Res.* **2005**, *38*, 624.
(36) Custelcean, R.; Jackson, J. E. Dihydrogen Bonding: Structures, Energetics, and Dynamics. *Chem. Rev.* **2001**, *101*, 1963.
(37) Padilla-Martińez, I. I.; Rosalez-Hoz, M. D. J.; Tlahuext, H.; Camacho-Camacho, C.; Ariza-Castolo, A.; Contreras, R. Azolylborane Adducts. Structural and Conformational Analysis by X-ray Diffraction and NMR. Protic-Hydric ($C-H^{\delta+}-^{\delta-}H-B$) and Protic-Fluoride ($C-H^{\delta+}-^{\delta-}F-B$) Interactions. *Chem. Ber.* **1996**, *129*, 441.
(38) Filippov, O. A.; Belkova, N. V.; Epstein, L. M.; Shubina, E. S. Chemistry of Boron Hydrides Orchestrated by Dihydrogen Bonds. *J. Organomet. Chem.* **2013**, *747*, 30.
(39) Custelcean, R.; Jackson, J. E. Topochemical Dihydrogen to Covalent Bonding Transformation in $LiBH_4$ TEA: A Mechanistic Study. *J. Am. Chem. Soc.* **2000**, *122*, 5251.
(40) Custelcean, R.; Jackson, J. E. Topochemical Control of Covalent Bond Formation by Dihydrogen Bonding. *J. Am. Chem. Soc.* **1998**, *120*, 12935.
(41) Gatling, S. C.; Jackson, J. E. Reactivity Control Via Dihydrogen Bonding: Diastereoselection in Borohydride Reductions of A-Hydroxyketones. *J. Am. Chem. Soc.* **1999**, *121*, 8655.
(42) Marincean, S.; Fritz, M.; Scamp, R.; Jackson, J. E. Mechanistic Investigations in A-Hydroxycarbonyls Reduction by BH_4. *J. Phys. Org. Chem.* **2012**, *25*, 1186.
(43) Amendola, S. C.; Sharp-Goldman, S. L.; Janjua, M. S.; Spencer, N. C.; Kelly, M. T.; Petillo, P. J.; Binder, M. A Safe, Portable, Hydrogen Gas Generator Using Aqueous Borohydride Solution and Ru Catalyst. *Int. J. Hydrogen Energy* **2000**, *25*, 969.
(44) Concha, B. M.; Chatenet, M.; Coutanceau, C.; Hahn, F. In Situ Infrared (FTIR) Study of the Borohydride Oxidation Reaction. *Electrochem. Commun.* **2009**, *11*, 223.
(45) Filinchuk, Y.; Hagemann, H. Structure and Properties of $NaBH_4{\cdot}2H_2O$ and $NaBH_4$. *Eur. J. Inorg. Chem.* **2008**, *2008*, 3127.
(46) Duffin, A. M.; England, A. H.; Schwartz, C. P.; Uejio, J. S.; Dallinger, G. C.; Shih, O.; Prendergast, D.; Saykally, R. J. Electronic Structure of Aqueous Borohydride: A Potential Hydrogen Storage Medium. *Phys. Chem. Chem. Phys.* **2011**, *13*, 17077.
(47) Asbury, J. B.; Steinel, T.; Stromberg, C.; Corcelli, S. A.; Lawrence, C. P.; Skinner, J. L.; Fayer, M. D. Water Dynamics: Vibrational Echo Correlation Spectroscopy and Comparison to Molecular Dynamics Simulations. *J. Phys. Chem. A* **2004**, *108*, 1107.
(48) Bakker, H. J.; Skinner, J. L. Vibrational Spectroscopy as a Probe of Structure and Dynamics in Liquid Water. *Chem. Rev.* **2010**, *110*, 1498.
(49) Bakker, H. J.; Woutersen, S.; Nienhuys, H. K. Reorientational Motion and Hydrogen-Bond Stretching Dynamics in Liquid Water. *Chem. Phys.* **2000**, *258*, 233.
(50) Fecko, C. J.; Loparo, J. J.; Roberts, S. T.; Tokmakoff, A. Local Hydrogen Bonding Dynamics and Collective Reorganization in Water: Ultrafast Infrared Spectroscopy of HOD/D_2O. *J. Chem. Phys.* **2005**, *122*, 054506.
(51) Laage, D.; Hynes, J. T. On the Molecular Mechanism of Water Reorientation. *J. Phys. Chem. B* **2008**, *112*, 14230.
(52) Roberts, S. T.; Ramasesha, K.; Tokmakoff, A. Structural Rearrangments in Water Viewed through Two-Dimensional Infrared Spectroscopy. *Acc. Chem. Res.* **2009**, *42*, 1239.
(53) Steinel, T.; Asbury, J. B.; Corcelli, S. A.; Lawrence, C. P.; Skinner, J. L.; Fayer, M. D. Water Dynamics: Dependence on Local Structure Probed with Vibrational Echo Correlation Spectroscopy. *Chem. Phys. Lett.* **2004**, *386*, 295.
(54) Steinel, T.; Asbury, J. B.; Zheng, J. R.; Fayer, M. D. Watching Hydrogen Bonds Break: A Transient Absorption Study of Water. *J. Phys. Chem. A* **2004**, *108*, 10957.
(55) Stenger, J.; Madsen, D.; Hamm, P.; Nibbering, E. T. J.; Elsaesser, T. A Photon Echo Peak Shift Study of Liquid Water. *J. Phys. Chem. A* **2002**, *106*, 2341.
(56) Asbury, J. B.; Steinel, T.; Kwak, K.; Corcelli, S. A.; Lawrence, C. P.; Skinner, J. L.; Fayer, M. D. Dynamics of Water Probed with Vibrational Echo Correlation Spectroscopy. *J. Chem. Phys.* **2004**, *121*, 12431.
(57) Woutersen, S.; Emmerichs, U.; Bakker, H. J. Femtosecond Mid-IR Pump-Probe Spectroscopy of Liquid Water: Evidence for a Two-Component Structure. *Science* **1997**, *278*, 658.
(58) Gaffney, K. J.; Piletic, I. R.; Fayer, M. D. Orientational Relaxation and Vibrational Excitation Transfer in Methanol−Carbon Tetrachloride Solutions. *J. Chem. Phys.* **2003**, *118*, 2270.
(59) Cowan, M. L.; Bruner, B. D.; Huse, N.; Dwyer, J. R.; Chugh, B.; Nibbering, E. T. J.; Elsaesser, T.; Miller, R. J. D. Ultrafast Memory Loss and Energy Redistribution in the Hydrogen Bond Network of Liquid H_2O. *Nature* **2005**, *434*, 199.
(60) Rosenfeld, D. E.; Fayer, M. D. Excitation Transfer Induced Spectral Diffusion and the Influence of Structural Spectral Diffusion. *J. Chem. Phys.* **2012**, *137*, 064109.
(61) Nishida, J.; Fei, H.; Tamimi, A.; Pullen, S.; Ott, S.; Cohen, S. M.; Fayer, M. D. Structural Dynamics inside a Functionalized Metal−Organic Framework Probed by Ultrafast 2D-IR Spectroscopy. *Proc. Natl. Acad. Sci. U.S.A.* **2014**, *111*, 18442.
(62) Woutersen, S.; Bakker, H. J. Resonant Intermolecular Transfer of Vibrational Energy in Liquid Water. *Nature* **1999**, *402*, 507.
(63) Corcelli, S. A.; Lawrence, C. P.; Asbury, J. B.; Steinel, T.; Fayer, M. D.; Skinner, J. L. Spectral Diffusion in a Fluctuating Charge Model of Water. *J. Chem. Phys.* **2004**, *121*, 8897.
(64) Fenn, E. E.; Wong, D. B.; Fayer, M. D. Water Dynamics in Small Reverse Micelles in Two Solvents: Two-Dimensional Infrared Vibrational Echoes with Two-Dimensional Background Subtraction. *J. Chem. Phys.* **2011**, *134*, 054512.
(65) Yu, L.; Matthews, M. A. Hydrolysis of Sodium Borohydride in Concentrated Aqueous Solution. *Int. J. Hydrogen Energy* **2011**, *36*, 7416.
(66) Kreevoy, M. M.; Jacobson, R. W. The Rate of Decomposition of $NaBH_4$ in Basic Aqueous Solutions. *Ventron Alembic.* **1979**, *15*, 2.
(67) Park, S.; Fayer, M. D. Hydrogen Bond Dynamics in Aqueous Nabr Solutions. *Proc. Natl. Acad. Sci. U.S.A.* **2007**, *104*, 16731.
(68) Singh, P. C.; Patwari, G. N. Proton Affinity Correlations between Hydrogen and Dihydrogen Bond Acceptors. *J. Phys. Chem. A* **2007**, *111*, 3178.
(69) Law, J. K.; Mellows, H. M.; Heinekey, D. M. H−H Distances in Elongated Transition Metal Dihydrogen Complexes: Effects of Temperature and Isotopic Substitution. *Abstracts of Papers, 221st ACS National Meeting, San Diego, CA, United States, April 1−5, 2001*, 2001, INOR.
(70) McDowell, S. A. C.; Forde, T. S. Isotope Effects in Linear Dihydrogen Bonded Complexes Containing Lih. *J. Chem. Phys.* **2002**, *117*, 6032.
(71) Nakai, H.; Ikabata, Y.; Tsukamoto, Y.; Imamura, Y.; Miyamoto, K.; Hoshino, M. Isotope Effect in Dihydrogen-Bonded Systems: Application of the Analytical Energy Gradient Method in the Nuclear Orbital Plus Molecular Orbital Theory. *Mol. Phys.* **2007**, *105*, 2649.
(72) Ketelaar, J. A. A.; Schutte, C. J. H. The Borohydride Ion (BH_4^-) in a Face-Centred Cubic Alkali-Halide Lattice. *Spectrochim. Acta* **1961**, *17*, 1240.
(73) Schutte, C. J. H. The Infra-Red Spectrum of Thin Films of Sodium Borohydride. *Spectrochim. Acta* **1960**, *16*, 1054.
(74) Emery, A. R.; Taylor, R. C. Raman Spectroscopy in Liquid Ammonia Solutions. Vibrational Frequencies and Force Constants for Isotopic Species of the Borohydride Ion Having Tetrahedral Symmetry. *J. Chem. Phys.* **1958**, *28*, 1029.
(75) Roberts, S. T.; Petersen, P. B.; Ramasesha, K.; Tokmakoff, A.; Ufimtsev, I. S.; Martinez, T. J. Observation of a Zundel-Like Transition

DOI: 10.1021/jp512426y
J. Phys. Chem. B 2015, 119, 3546−3559

State During Proton Transfer in Aqueous Hydroxide Solutions. *Proc. Natl. Acad. Sci. U. S. A.* **2009**, *106*, 15154.
(76) Roberts, S. T.; Ramasesha, K.; Petersen, P. B.; Mandal, A.; Tokmakoff, A. Proton Transfer in Concentrated Aqueous Hydroxide Visualized Using Ultrafast Infrared Spectroscopy. *J. Phys. Chem. A* **2011**, *115*, 3957.
(77) Hunger, J.; Liu, L.; Tielrooij, K.-J.; Bonn, M.; Bakker, H. Vibrational and Orientational Dynamics of Water in Aqueous Hydroxide Solutions. *J. Chem. Phys.* **2011**, *135*.
(78) Liu, L.; Hunger, J.; Bakker, H. J. Energy Relaxation Dynamics of the Hydration Complex of Hydroxide. *J. Phys. Chem. A* **2011**, *115*, 14593.
(79) Rezus, Y. L. A.; Bakker, H. J. On the Orientational Relaxation of HDO in Liquid Water. *J. Chem. Phys.* **2005**, *123*, 114502.
(80) Moilanen, D. E.; Fenn, E. E.; Wong, D.; Fayer, M. D. Water Dynamics in Large and Small Reverse Micelles: From Two Ensembles to Collective Behavior. *J. Chem. Phys.* **2009**, *131*, 014704.
(81) Moilanen, D. E.; Fenn, E. E.; Wong, D.; Fayer, M. D. Water Dynamics at the Interface in AOT Reverse Micelles. *J. Phys. Chem. B* **2009**, *113*, 8560.
(82) Kenkre, V. M.; Tokmakoff, A.; Fayer, M. D. Theory of Vibrational Relaxation of Polyatomic Molecules in Liquids. *J. Chem. Phys.* **1994**, *101*, 10618.
(83) Egorov, S. A.; Berne, B. J. Vibrational Energy Relaxation in the Condensed Phases: Quantum vs. Classical Bath for Multiphonon Processes. *J. Chem. Phys.* **1997**, *107*, 6050.
(84) Kropman, M. F.; Bakker, H. J. Effect of Ions on the Vibrational Relaxation of Liquid Water. *J. Am. Chem. Soc.* **2004**, *126*, 9135.
(85) Kwak, K.; Park, S.; Finkelstein, I. J.; Fayer, M. D. Frequency-Frequency Correlation Functions and Apodization in 2D-IR Vibrational Echo Spectroscopy, a New Approach. *J. Chem. Phys.* **2007**, *127*, 124503.
(86) Kwak, K.; Rosenfeld, D. E.; Fayer, M. D. Taking Apart the Two-Dimensional Infrared Vibrational Echo Spectra: More Information and Elimination of Distortions. *J. Chem. Phys.* **2008**, *128*, 204505.
(87) Fenn, E. E.; Fayer, M. D. Extracting 2D-IR Frequency-Frequency Correlation Functions from Two Component Systems. *J. Chem. Phys.* **2011**, *135*, 07450.
(88) Berry, R. S.; Rice, S. A.; Ross, J. *Physical Chemistry*; Oxford University Press: New York, 2000.
(89) Tokmakoff, A.; Urdahl, R. S.; Zimdars, D.; Francis, R. S.; Kwok, A. S.; Fayer, M. D. Vibrational Spectral Diffusion and Population-Dynamics in a Glass-Forming Liquid - Variable Bandwidth Picosecond Infrared-Spectroscopy. *J. Chem. Phys.* **1995**, *102*, 3919.
(90) Eaves, J. D.; Tokmakoff, A.; Geissler, P. L. Electric Field Fluctuations Drive Vibrational Dephasing in Water. *J. Phys. Chem. A* **2005**, *109*, 9424.
(91) Williams, R. B.; Loring, R. F.; Fayer, M. D. Vibrational Dephasing of Carbonmonoxy Myoglobin. *J. Phys. Chem. B* **2001**, *105*, 4068.
(92) Bagchi, S.; Nebgen, B. T.; Loring, R. F.; Fayer, M. D. Dynamics of a Myoglobin Mutant Enzyme: 2D-IR Vibrational Echo Experiments and Simulations. *J. Am. Chem. Soc.* **2010**, *132*, 18367.
(93) Bagchi, S.; Boxer, S. G.; Fayer, M. D.; Ribonuclease, S. Dynamics Measured Using a Nitrile Label with 2D-IR Vibrational Echo Spectroscopy. *J. Phys. Chem. B* **2012**, *116*, 4034.
(94) Moilanen, D. E.; Fenn, E. E.; Lin, Y. S.; Skinner, J. L.; Bagchi, B.; Fayer, M. D. Water Inertial Reorientation: Hydrogen Bond Strength and the Angular Potential. *Proc. Natl. Acad. Sci. U.S.A.* **2008**, *105*, 5295.
(95) Tuckerman, M. E.; Chandra, A.; Marx, D. Structure and Dynamics of OH^-(Aq). *Acc. Chem. Res.* **2006**, *39*, 151.
(96) Zheng, J.; Kwak, K.; Asbury, J. B.; Chen, X.; Piletic, I. R.; Fayer, M. D. Ultrafast Dynamics of Solute-Solvent Complexation Observed at Thermal Equilibrium in Real Time. *Science* **2005**, *309*, 1338.
(97) Krekeler, C.; Hess, B.; Site, L. D. Density Functional Study of Ion Hydration for the Alkali Metal Ions (Li^+, Na^+, K^+) and the Halide Ions (F^-, Br^-, Cl^-). *J. Chem. Phys.* **2006**, *125*, 054305.
(98) Laage, D.; Hynes, J. T. A Molecular Jump Mechanism of Water Reorientation. *Science* **2006**, *311*, 832.

DOI: 10.1021/jp512426y
J. Phys. Chem. B 2015, 119, 3546−3559